Article

Cell Reports

TNF-Mediated Restriction of Arginase 1 Expression in Myeloid Cells Triggers Type 2 NO Synthase Activity at the Site of Infection

Graphical Abstract

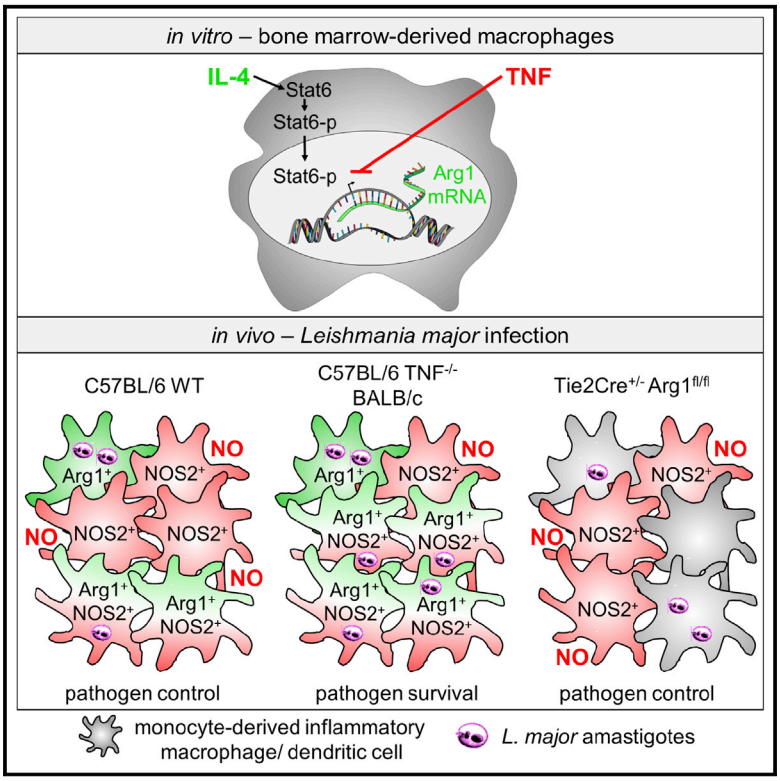

Authors

Ulrike Schleicher, Katrin Paduch, Andrea Debus, ..., Renato Ostuni, Heinrich Körner, Christian Bogdan

Correspondence

christian.bogdan@uk-erlangen.de

In Brief

Control of intracellular pathogens requires TNF, but its mechanism of action is incompletely understood. Schleicher et al. show that TNF suppresses Arg1 expression in myeloid cells by decreasing histone acetylation, resulting in enhanced production of NO by NOS2 in situ. Arg1 deletion rescues *Leishmania*-infected mice from a non-healing infection.

Highlights

- TNF inhibits IL-4-induced Arg1 expression in macrophages and dendritic cells
- Arg1 is upregulated in macrophages or dendritic cells of *L. major*-infected $TNF^{-/-}$ mice
- Arg1 hyperexpression in $TNF^{-/-}$ mice impairs in situ production of leishmanicidal NO
- Arg1 deletion restores parasite and disease control in otherwise non-healing mice

Schleicher et al., 2016, Cell Reports *15*, 1062–1075
May 3, 2016 ©2016 The Authors
http://dx.doi.org/10.1016/j.celrep.2016.04.001

OPEN ACCESS
CellPress

Cell Reports
Article

TNF-Mediated Restriction of Arginase 1 Expression in Myeloid Cells Triggers Type 2 NO Synthase Activity at the Site of Infection

Ulrike Schleicher,[1,2,10] Katrin Paduch,[1,10] Andrea Debus,[1,10] Stephanie Obermeyer,[1] Till König,[3,12] Jessica C. Kling,[4,13] Eliana Ribechini,[5] Diana Dudziak,[2,6] Dimitrios Mougiakakos,[2,7] Peter J. Murray,[8] Renato Ostuni,[9,14] Heinrich Körner,[4,11] and Christian Bogdan[1,2,11,*]

[1]Mikrobiologisches Institut-Klinische Mikrobiologie, Immunologie und Hygiene, Friedrich-Alexander-Universität (FAU) Erlangen-Nürnberg and Universitätsklinikum Erlangen, 91054 Erlangen, Germany
[2]Medical Immunology Campus Erlangen, FAU Erlangen-Nürnberg, 91054 Erlangen, Germany
[3]Abteilung Mikrobiologie und Hygiene, Institut für Medizinische Mikrobiologie und Hygiene, Albert-Ludwigs-Universität Freiburg, 79104 Freiburg, Germany
[4]Menzies Institute for Medical Research Tasmania, Hobart, Tasmania 7000, Australia
[5]Institute of Virology and Immunobiology, University of Würzburg, 97078 Würzburg, Germany
[6]Laboratory of DC Biology, Department of Dermatology, FAU Erlangen-Nürnberg and Universitätsklinikum Erlangen, 91054 Erlangen, Germany
[7]Department of Internal Medicine 5, Hematology and Oncology, FAU Erlangen-Nürnberg and Universitätsklinikum Erlangen, 91054 Erlangen, Germany
[8]Departments of Infectious Diseases and Immunology, St. Jude Children's Research Hospital, Memphis, TN 38105, USA
[9]Department of Experimental Oncology, European Institute of Oncology (IEO), 20139 Milan, Italy
[10]Co-first author
[11]Co-senior author
[12]Present address: Biologicals Quality, Novartis Pharma, CH-4002 Basel, Switzerland
[13]Present address: The University of Queensland Diamantina Institute, Translational Research Institute, Woolloongabba Queensland 4102, Australia
[14]Present address: San Raffaele Telethon Institute for Gene Therapy (SR-TIGET) and Division of Regenerative Medicine, Stem Cells and Gene Therapy, San Raffaele Scientific Institute, 20132 Milano, Italy
*Correspondence: christian.bogdan@uk-erlangen.de
http://dx.doi.org/10.1016/j.celrep.2016.04.001

SUMMARY

Neutralization or deletion of tumor necrosis factor (TNF) causes loss of control of intracellular pathogens in mice and humans, but the underlying mechanisms are incompletely understood. Here, we found that TNF antagonized alternative activation of macrophages and dendritic cells by IL-4. TNF inhibited IL-4-induced arginase 1 (Arg1) expression by decreasing histone acetylation, without affecting STAT6 phosphorylation and nuclear translocation. In *Leishmania major*-infected C57BL/6 wild-type mice, type 2 nitric oxide (NO) synthase (NOS2) was detected in inflammatory dendritic cells or macrophages, some of which co-expressed Arg1. In TNF-deficient mice, Arg1 was hyperexpressed, causing an impaired production of NO in situ. A similar phenotype was seen in *L. major*-infected BALB/c mice. Arg1 deletion in hematopoietic cells protected these mice from an otherwise lethal disease, although their disease-mediating T cell response (Th2, Treg) was maintained. Thus, deletion or TNF-mediated restriction of Arg1 unleashes the production of NO by NOS2, which is critical for pathogen control.

INTRODUCTION

Myeloid cells such as macrophages play pivotal roles in the immune system. They are essential for the uptake, killing, and degradation of pathogens, the processing and presentation of antigens, and the activation of effector T cell populations but also for the termination of T cell responses, the resolution of inflammatory processes, and for tissue homeostasis. The functional diversity of macrophages largely results from exposure to different microenvironmental cues, including cytokines and tissue-specific signals (Ginhoux et al., 2015; Lavin et al., 2014). Whereas interferon (IFN)-γ and tumor necrosis factor (TNF) are associated with the induction of classically activated or M1-like macrophages expressing anti-microbial effector functions, cytokines such as interleukin (IL)-4, IL-10, IL-13, or transforming growth factor (TGF)-β limit the release of proinflammatory factors by macrophages and promote macrophage phenotypes that suppress T cell responses and/or support tissue repair (Ginhoux et al., 2015). These macrophages, which were operationally dubbed suppressor (Kirchner et al., 1975), deactivated (Tsunawaki and Nathan, 1986), alternatively activated (Stein et al.,

1992), or M2 (Mills et al., 2000), depending on their exact secretory and immunomodulatory function and surface phenotype, are characterized by distinct transcriptional and proteomic profiles (Murray et al., 2014). IL-4, for example, causes upregulation of the mannose receptor 1 (*Mrc1*; CD206), the chitinase-3-like-protein 3 (*Ym1*, *Chi3l3*), the resistin-like molecule alpha (Relma, *Retnla*; also termed "found in inflammatory zone-1" [*Fizz1*]), macrophage galactose-type C-type lectin 2 (*Mgl2*; CD301b), programmed death ligand 2 (*Pdl2*; CD273), or arginase 1 (*Arg1*).

Arg1 is a cytosolic enzyme that hydrolyzes L-arginine into urea and ornithine. It is a constitutive and essential component of the hepatic urea cycle, which explains the postnatal lethality of *Arg1*$^{-/-}$ mice (Iyer et al., 2002), but it is inducible in many other cell types, including macrophages and endothelial and epithelial cells (Morris, 2009). In the immune system, arginine metabolism by Arg1 has been conceptually linked to three major processes. First, because ornithine is a precursor of the polyamines or proline required for cell proliferation or collagen synthesis, respectively, Arg1 expression is characteristic for wound healing and tissue regeneration, whereas excessive Arg1 activity can cause organ fibrosis (Wynn et al., 2013). Second, Arg1 expression by suppressor myeloid cells might deprive T cells of arginine and thereby impair their activation and proliferation during anti-infectious or anti-tumor immune responses (Bogdan, 2015; Pesce et al., 2009). Third, Arg1 competes with inducible nitric oxide (NO) synthase (iNOS) or type 2 NO synthase (NOS2), a key anti-microbial and immunoregulatory pathway, for the common substrate L-arginine (Bogdan, 2015; El-Gayar et al., 2003; Rutschman et al., 2001). Accordingly, Arg1 activity is correlated with increased pathogen loads in infectious diseases (De Muylder et al., 2013; Iniesta et al., 2005; Kropf et al., 2005). However, Arg1 was also observed to limit immunopathology and fibrosis (Pesce et al., 2009) and to prevent microbial growth, notably in the absence of NOS2 activity (Duque-Correa et al., 2014).

Due to the diverse and possibly pathological effects of Arg1, its expression requires tight control. In the past, research focused on defining factors that upregulate Arg1. Several studies revealed that not only cytokines but also microbes or microbial products (De Muylder et al., 2013; El Kasmi et al., 2008), hypoxia, or lactic acid (Colegio et al., 2014; Louis et al., 1998) induced Arg1. In contrast, the negative regulation of Arg1 in situ during infections has not yet been addressed.

TNF is essential for the defense against intracellular microorganisms and for maintaining lifelong control of latent pathogens. Experiments with anti-TNF antibodies, tumor necrosis factor receptor (TNFR)$^{-/-}$, or *Tnf*$^{-/-}$ mouse strains, as well as treatment of humans suffering from autoimmune diseases with TNF antagonists, have demonstrated the protective role of TNF (Allenbach et al., 2008; Flynn et al., 1995; Grivennikov et al., 2005; Marino et al., 1997; Novosad and Winthrop, 2014; Pfeffer et al., 1993; Vassalli, 1992). However, the TNF-mediated molecular mechanisms of pathogen control in vivo are still poorly defined. *Tnf*$^{-/-}$ C57BL/6 mice locally infected with the protozoan parasite *Leishmania major* (FEBNI strain) succumbed to progressive cutaneous and visceral disease (Wilhelm et al., 2001). Unexpectedly, the development of type 1 T helper (Th1) cells and the expression of NOS2, which are strictly required for the resolution of *Leishmania* infections (Diefenbach et al., 1998; Liew et al., 1990), were preserved in *Tnf*$^{-/-}$ mice (Wilhelm et al., 2001), leading to interest in identifying the mechanism that underlies the exquisite susceptibility of this mouse strain.

Here, we tested the hypothesis that TNF causes protection by inhibiting the expression of Arg1 and the development of alternatively activated macrophages. We observed a strong negative regulatory effect of TNF on Arg1 expression in macrophages and dendritic cells. In *L. major*-infected wild-type (WT) mice, Arg1 was weakly expressed. In *Tnf*$^{-/-}$ mice, Arg1 was strongly upregulated, leading to a frequent co-expression of Arg1 and NOS2 in monocyte-derived dendritic cells or macrophages. This impeded the production of NO in situ, a phenotype that was shared by highly susceptible BALB/c mice. Cell-type-specific deletion of Arg1 prevented an otherwise lethal course of infection.

RESULTS

TNF Inhibits the IL-4-Induced Expression of Arg1 and Other M2 Markers

We first tested the effect of TNF on the IL-4-induced Arg1 expression in bone marrow-derived macrophages (BMMs) and bone marrow-derived dendritic cells (BMDCs). Simultaneous addition of TNF caused downregulation of Arg1 mRNA and protein in BMMs (Figures 1A–1C). The suppression of Arg1 protein was more prominent at higher TNF/IL-4 ratios (Figure S1A), except for IL-4 concentrations ($\leq$1 ng/ml) that were too low to induce Arg1 protein above control levels (Figures S1B and S1C). In time course experiments, the inhibitory effect of TNF was noticeable once Arg1 mRNA or protein was induced by IL-4 above the level of unstimulated cells (Figures 1D and 1E). TNF alone induced NOS2 mRNA in BMMs and, at high concentrations, NOS2 protein and activity (Figures 1A, 1B, 1E, and 1F).

The suppressive activity of TNF on IL-4-triggered Arg1 expression was largely independent of NOS2-derived NO (Figure S1D), maintained in macrophages that were infected with *L. major* (Figure S1E), and observed with BMDCs (Figures 1F and S1C) and resident peritoneal macrophages (data not shown). In both BMMs and BMDCs, the effect was somewhat more pronounced when the cells were derived from *Tnf*$^{-/-}$ mice (Figures 1F and S1C); cultures from *Tnf*$^{-/-}$ BMDCs, however, did not differ from WT BMDCs in the total yield of cells, the dendritic cell maturation state (expression of CD40, CD80, CD86, and major histocompatibility complex [MHC] class II) or the expression of TNFR1 (CD120a) and TNFR2 (CD120b) (data not shown).

In addition to Arg1, TNF antagonized the IL-4-mediated mRNA upregulation of the M2 markers *Retnla* and *Ym1*, whereas others (*Mgl2*, *Mrc1*) were not affected (Figure S1F). To further corroborate that TNF counteracts the development of M2 macrophages, we analyzed the metabolism of BMMs. As expected (Huang et al., 2014; Vats et al., 2006), IL-4 caused a shift toward mitochondrial oxidative phosphorylation via upregulation of the transcriptional PPARγ-coactivator-1β (PGC-1β), leading to a marked rise of the maximal oxygen consumption rate (OCR). TNF-stimulated BMMs, in contrast, showed an increased extracellular acidification rate (ECAR), indicating that they rely on aerobic glycolysis. Simultaneous addition of IL-4 and TNF to unbiased

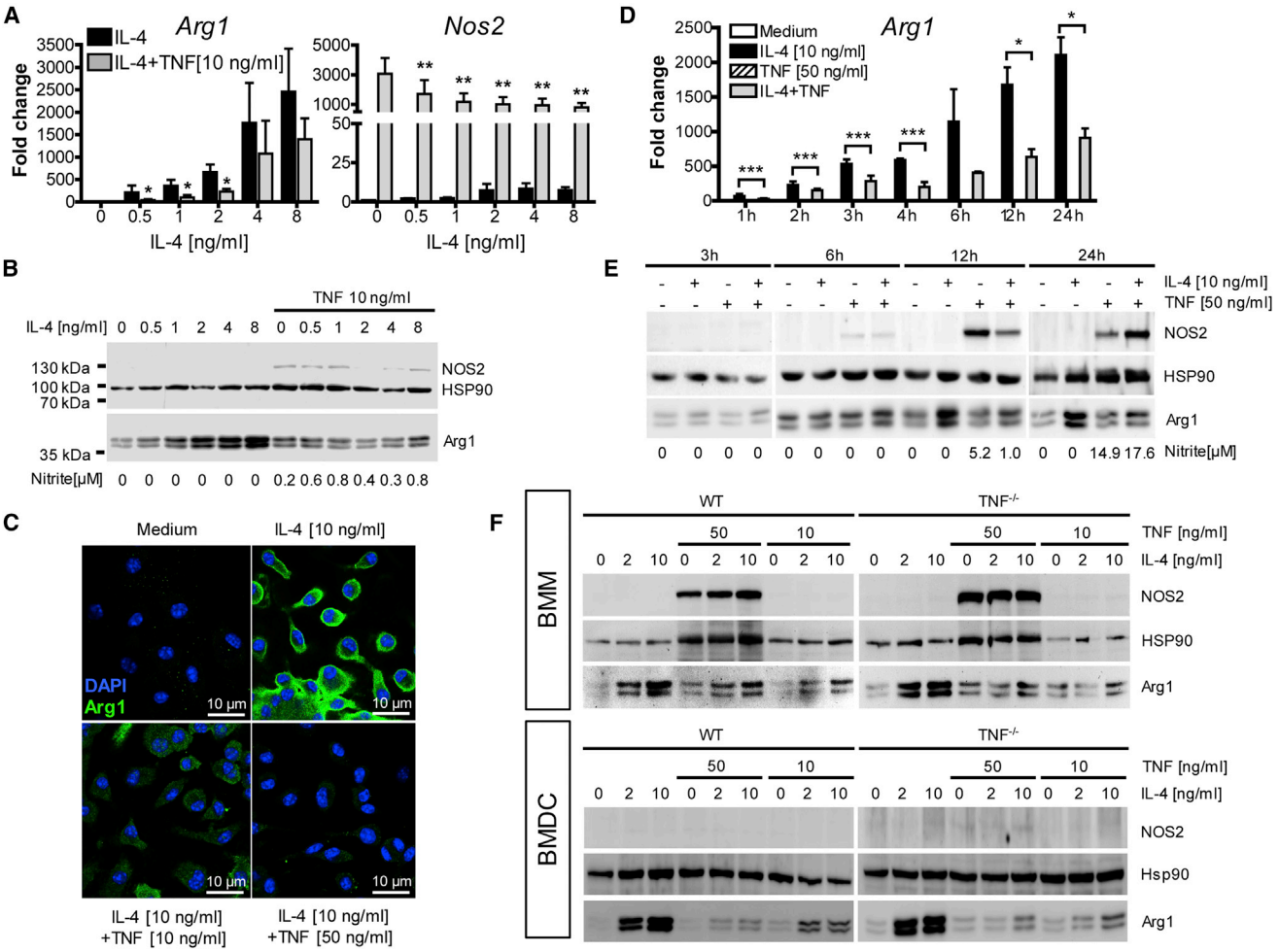

Figure 1. TNF Inhibits the Expression of Arg1 in BMMs and BMDCs

(A–F) BMMs (A–F) or BMDCs (F) of C57BL/6 WT (A–E) or *Tnf*$^{-/-}$ mice (F) were cultured with or without IL-4 (0.5–10 ng/ml) or TNF (10 or 50 ng/ml) for 1–24 hr, followed by the determination of NO_2^- in the supernatants (B and E). (A and D) A qRT-PCR analysis of BMMs. Results were calibrated to the medium value and represent means ± SEM of six to eight (A) or two to four (D) experiments. *$p < 0.05$; **$p < 0.01$; ***$p < 0.005$, two-tailed Mann-Whitney U test comparing IL-4 ± TNF. (B, E, and F) Western blot analysis of BMMs or BMDCs. One of three (B), two (E), or four (F) experiments. (C) CLSFM of BMMs. One of three experiments. See also Figures S1A–S1F.

BMMs prevented the induction of *Pgc-1β* mRNA by IL-4 and the subsequent metabolic changes (Figures 2A and 2B).

Because the IL-4-induced expression of *Arg1* and *Pgc-1β* strictly depends on Stat6 (Rutschman et al., 2001; Vats et al., 2006), we thought that TNF inhibited the Stat6 pathway. However, TNF neither suppressed the phosphorylation (Figures 2C and 2D) nor the nuclear translocation of signal transducer and activator of transcription 6 (STAT6) (Figure 2E). Furthermore, TNF did not affect the stability of *Arg1* mRNA (data not shown). To explore whether TNF might act by diminishing the accessibility of transcription factors to the *Arg1* promoter and enhancer regions, we performed chromatin immunoprecipitations (ChIPs) using an antibody against acetylated lysine 27 of histone H3 (H3K27ac). This histone mark is highly enriched at active *cis*-regulatory regions (promoters and enhancers) and directly correlates with chromatin accessibility and transcription of the target gene (Creyghton et al., 2010; Rada-Iglesias et al., 2011). In line with previous results (Ostuni et al., 2013), stimulation of BMMs with IL-4 triggered a rapid and persistent gain of H3 acetylation at *Arg1* promoter and putative enhancer sites (see Supplemental Information). Co-administration of TNF to IL-4-stimulated cultures markedly reduced the histone acetylation. TNF-mediated inhibition of H3 acetylation was maximal at 4 hr and correlated well with the reduction of *Arg1* mRNA at the same time point (Figures 2F and S1G).

Thus, TNF counteracts various components of the IL-4-driven activation of myeloid cells. This appears to be at least partly due to an impaired opening of the chromatin, as demonstrated for the *Arg1* promoter and enhancer elements.

Arg1 and Other M2 Marker Are Upregulated in *Tnf*$^{-/-}$ Mice

To address whether the TNF-mediated suppression of Arg1 also occurred in vivo, we used the C57BL/6 *L. major* infection

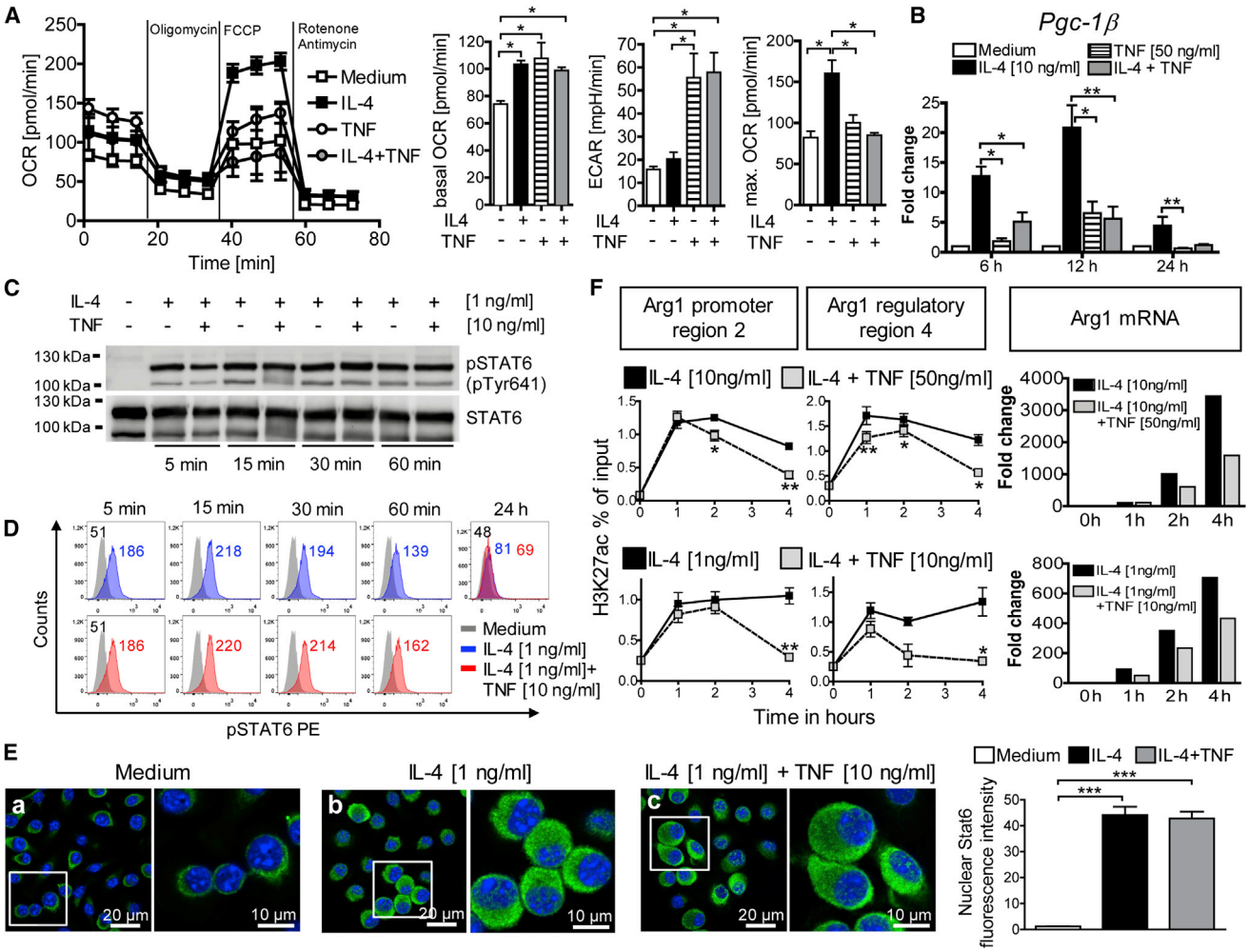

Figure 2. TNF Suppresses IL-4-Induced Oxidative Phosphorylation and Histone Acetylation but Does Not Affect Activation and Translocation of STAT6

C57BL/6 BMMs were cultured with or without IL-4 ± TNF for 5 min to 24 hr.

(A) The 24-hr cultures of stimulated BMMs (10 ng/ml IL-4; 50 ng/ml TNF) were analyzed for basal OCR and ECAR. In addition, the OCR response to oligomycin (ATP synthase inhibitor), carbonyl cyanide p-trifluoromethoxyphenylhydrazone (FCCP) (uncoupler), or rotenone or anti-mycin (electron transport inhibitors) was measured. One of four experiments (left). Bar graph panels show means ± SEM of basal OCR, ECAR, and maximal OCR.

(B) A qRT-PCR analysis. Means ± SEM calibrated to medium values of four experiments.

(C and D) STAT6 phosphorylation monitored by STAT6 immunoprecipitation (followed by western blot of pSTAT6 [pTyr641] and reprobing of total STAT6 protein; C) or by flow cytometry (D). In a parallel western blot, suppression of IL-4-induced Arg1 by TNF was ascertained after 24 hr (not shown). One of five experiments.

(E) Nuclear translocation of STAT6 protein in BMMs after 3 hr of stimulation, visualized by CLSFM after staining with Alexa Fluor 488-conjugated anti-STAT6 (green) and DAPI (nuclei, blue). One of three experiments. Quantification of nuclear STAT6 fluorescence intensity of 100 cells per condition from three experiments (right panel).

(F) H3K27ac-ChIP of fixed BMMs. Eluted and quantified DNA was subjected in duplicates to qPCR analysis using primer pairs spanning the Arg1 promoter region 2 or the putative regulatory or enhancer region 4 (see the Supplemental Experimental Procedures). Results of two experiments are shown as relative enrichment compared to 1% input DNA. Aliquots of the same BMM cultures were analyzed in parallel for Arg1 mRNA by qRT-PCR (right panel).

*p ≤ 0.05; **p ≤ 0.01; ***p < 0.005, ****p < 0.0001, two-tailed Mann-Whitney U test. See also Figure S1G.

model. The control of *L. major* FEBNI strain in C57BL/6 mice strictly required NOS2 and TNF (Diefenbach et al., 1998; Wilhelm et al., 2001). Confirming our earlier data (Wilhelm et al., 2001), C57BL/6 $Tnf^{-/-}$ mice infected with *L. major* showed more severe skin lesions and higher numbers of parasites at the site of infection and in the lymphatic organs compared to C57BL/6 WT controls (Figure S2A). We observed upregulation of the mRNA (Figure 3A), protein, and activity of Arg1 (Figure 3B and S2B–S2E) in the tissues of *L. major*-infected $Tnf^{-/-}$ mice. Skin lesions of WT mice contained substantially higher amounts of Arg1 than did draining lymph nodes (dLNs). Consequently, the differences in Arg1 expression between $Tnf^{-/-}$ and WT mice were more prominent in dLNs than at the site of infection. Unlike with Arg1, infected WT and $Tnf^{-/-}$

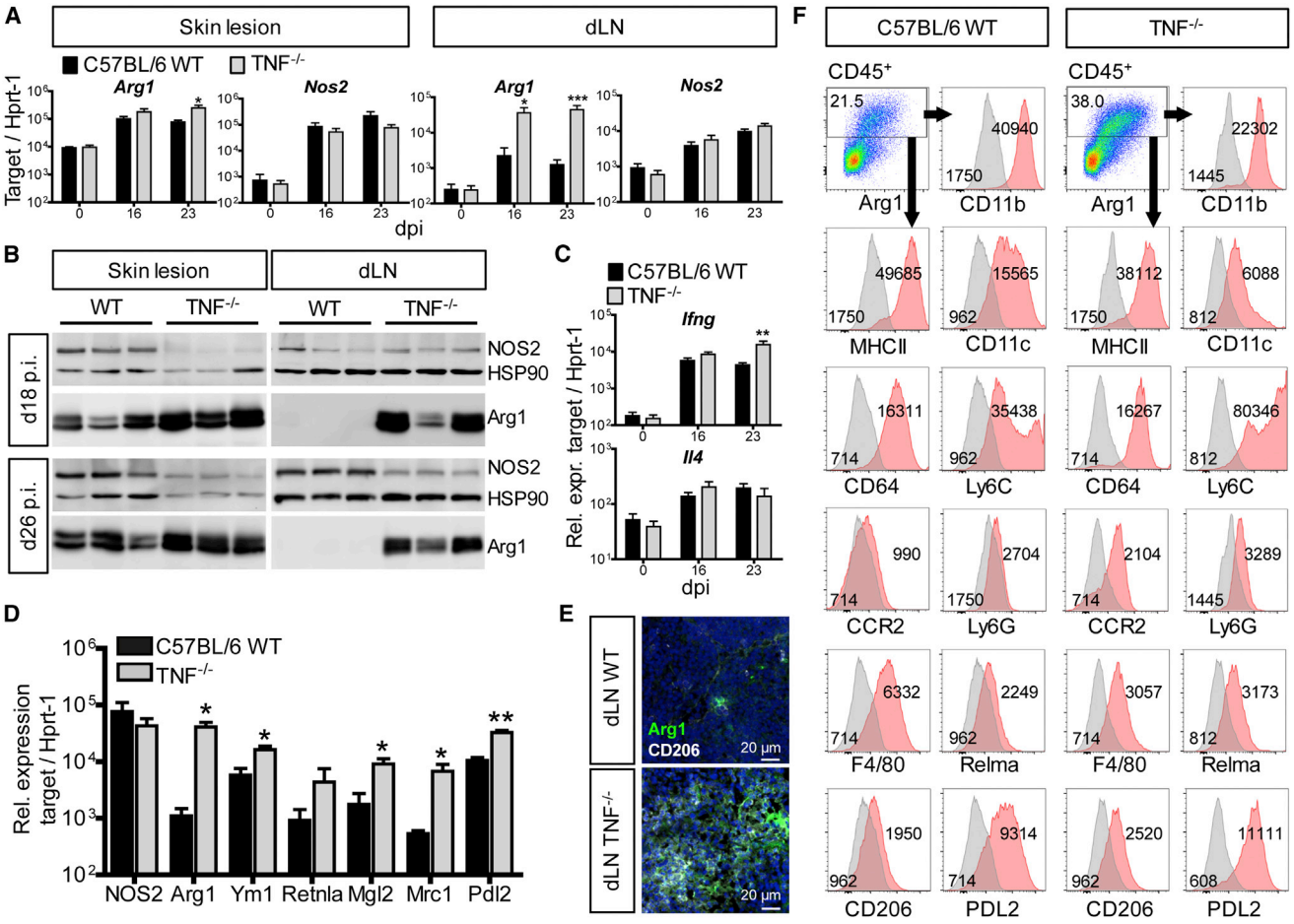

Figure 3. Arg1 and Other M2 Markers Are Upregulated in *L. major*-Infected *Tnf*$^{-/-}$ Mice

C57BL/6 WT and *Tnf*$^{-/-}$ mice were infected with *L. major*.

(A and C) qRT-PCR analysis of *Arg1* and *Nos2* in skin lesions and dLNs (A) or of *Ifng* and *Il4* in dLNs (C) at different days after infection (means ± SEM of four experiments, with two or three mice per group and time point).

(B) Western blot of skin lesions and dLNs. One of five experiments, with three or four mice per group and time point.

(D) A qRT-PCR analysis of CD11b^{+} cells sorted from dLNs (21–27 days post-infection [dpi]) (means ± SEM of three experiments, with four mice per group).

(E) CLSFM of dLN sections (18 dpi) stained with anti-Arg1 or anti-CD206 antibodies and DAPI (nuclei, blue). The image is representative of three or four mice per group and two experiments.

(F) Flow cytometry of cell suspensions of skin lesions (23–29 dpi) from two or three mice per group and time point, which were pooled before staining. Within viable CD45^{+} cells excluding doublets (Figure S3A) Arg1^{+} cells were gated (red) and analyzed for the expression of surface markers (red, surface marker; gray, isotype or fluorescence minus one control; number, mean fluorescence value). One of four experiments.

*$p < 0.05$; **$p < 0.01$; ***$p < 0.005$, two-tailed Mann-Whitney U test. See also Figure S2.

mice had similar amounts of *Nos2* mRNA in the skin lesions and dLNs (Figure 3A), whereas the expression of NOS2 protein in total organ lysates of *Tnf*$^{-/-}$ mice was tentatively (skin) or significantly (dLN) lower than in WT controls (Figures 3B and S2B).

The enhanced expression of Arg1 in *L. major*-infected *Tnf*$^{-/-}$ mice is unlikely to result from a cytokine imbalance in this mouse strain, because there was no significant increase of *Il4* or lack of *Ifng* mRNA in *Tnf*$^{-/-}$ compared to WT mice (Figure 3C). At later time points, the expression of *Ifng* was even enhanced in infected *Tnf*$^{-/-}$ mice, demonstrating that *Tnf*$^{-/-}$ mice were fully capable of mounting a Th1 response to the increased parasite burden.

In CD11b^{+} myeloid cells sorted from the dLNs of *Tnf*$^{-/-}$ mice at day 21 to day 27 of *L. major* infection, the expression of *Arg1* and of other genes related to alternatively activated macrophages (e.g., *Ym1* and *Mrc1*) was significantly upregulated, whereas the amounts of *Nos2* mRNA were comparable in *Tnf*$^{-/-}$ versus WT cells (Figure 3D). Confocal laser scanning fluorescence microscopy (CLSFM) analysis confirmed the increased Mrc1 (CD206) expression in *Tnf*$^{-/-}$ dLNs on the protein level (Figure 3E).

Together, these data show that TNF, apart from its participation in the induction of NOS2, restricts the in vivo expression of Arg1 and of other IL-4-dependent genes in myeloid cells.

Increased Frequency of Arg1$^+$NOS2$^+$ Myeloid Cells in *L. major*-Infected *Tnf*$^{-/-}$ Mice

In addition to myeloid cells, Arg1 and NOS2 can be expressed by endothelial cells and fibroblasts (Morris, 2009; Witte et al., 2002). To define the cell population that accounts for Arg1 expression in C57BL/6 WT and *Tnf*$^{-/-}$ mice during *L. major* infection, single-cell analyses using multicolor flow cytometry were performed (for the gating strategy, see Figure S3A). In the skin lesions of WT mice, Arg1 was detected in CD11b$^+$CD11c$^+$MHCII$^+$ cells that were stained for other surface molecules in different combinations, including at least two of the previously mentioned markers. Co-expression was seen for CD64, Ly6C, CCR2, Ly6G, F4/80, Relma, CD206, and PDL2 (Figure 3F). Arg1$^+$ cells were not detected in the CD45$^-$ population (Figure S3B). The specificity of Arg1 staining was verified by isotype controls and by the absence of Arg1$^+$ cells in Arg1-deficient C57BL/6 mice (Figures 3F and S3C). Although we cannot formally exclude the existence of subsets within the Arg1$^+$ cells (because not all markers were stained in one sample), our data strongly point to one major Arg1$^+$ cell population. The surface phenotype of the Arg1$^+$ cells in the skin lesions identifies them as monocyte-derived inflammatory cells and allows them to be categorized either as dendritic cells or as macrophages (Fromm et al., 2012; Gautier et al., 2012; Tamoutounour et al., 2013).

The surface markers of the Arg1$^+$ cells were identical in WT and *Tnf*$^{-/-}$ mice. However, in line with the mRNA analyses of sorted CD11b$^+$ cells (Figure 3D), the levels of M2 markers (Relma, CD206, PDL2) were considerably higher in Arg1$^+$ cells from *Tnf*$^{-/-}$ mice, as was the expression of Ly6C and CCR2, whereas CD11c and F4/80 were reduced on Arg1$^+$ cells from *Tnf*$^{-/-}$ mice compared to WT controls (Figure 3F). Notably, the overall percentage of Arg1$^+$ cells was 2.14 (±0.32)-fold greater in *Tnf*$^{-/-}$ lesions than in WT lesions (mean ± SD of three experiments) (Figure 3F), which corroborates our western blot and CLSFM data. In two *Tnf*$^{-/-}$ mice, we detected the same Arg1$^+$ cells in dLNs, but the weaker expression of Arg1 and the limited sensitivity of flow cytometry precluded their routine detection in this organ (data not shown).

Because the size, granularity, and surface phenotype of NOS2$^+$ cells (Figures S3A and S3D) and of Arg1$^+$ cells (Figures 3F and S3A) were similar, we specifically assessed the potential co-expression of Arg1 and NOS2. As depicted in Figure 4A, the CD11b$^+$ cell population of skin lesions from *Tnf*$^{-/-}$ mice contained 2.2 (±0.68)-fold fewer NOS2$^+$ cells than did WT lesions (mean ± SD of three experiments). In addition, almost all NOS2$^+$ cells from *Tnf*$^{-/-}$ mice, but only around 50% from WT mice, co-expressed Arg1, and the mean fluorescence signal for Arg1 was higher in NOS2$^+$ cells from skin lesions of *Tnf*$^{-/-}$ mice. Overall, the percentage of Arg1$^+$NOS2$^+$ cells was 2.42 (±0.7)-fold higher in *Tnf*$^{-/-}$ compared to WT mice (Figure 4A). Thus, the preponderance of single-positive NOS2$^+$ cells seen in the myeloid cell population of WT mice is shifted toward NOS2$^+$Arg1^{high} double-positive cells in the absence of TNF.

In activated macrophages, NOS2 activity is equally distributed between the cytosol and a vesicular compartment (Bogdan, 2015). We therefore investigated the extent to which NOS2 and Arg1 co-localize when induced in one cell. Super-resolution microscopy of NOS2$^+$Arg1$^+$ BMMs (stimulated with IL-4 plus IFN-γ/lipopolysaccharide [LPS]) revealed overlapping expression of NOS2 and Arg1 in the cytoplasm, whereas the punctate (vesicular) NOS2$^+$ structures remained Arg1 negative (Figure 4B).

Hyperexpression of Arg1 in *Tnf*$^{-/-}$ Mice Impairs the Production of NO

Arginine depletion by Arg1 can inhibit NO production (due to substrate competition) or even downregulate NOS2 protein (El-Gayar et al., 2003; Rutschman et al., 2001). Because Arg1 and NOS2 were co-expressed within the same cell, we tested whether Arg1 hyperexpression in *Tnf*$^{-/-}$ mice correlates with reduced activity of NOS2 in situ.

CLSFM analysis of skin lesions confirmed not only the presence of NOS2$^+$, Arg1$^+$, or NOS2$^+$Arg1$^+$ myeloid cells but also the substantially higher amounts of Arg1 (both in terms of cell number and MFI) and lower expression of NOS2 (cell number) in *Tnf*$^{-/-}$ mice compared to WT controls (Figures 4C, a versus b, and 4E; Figure S4A, a versus b). *Leishmania* parasites were preferentially found in Arg1$^+$ foci and were more abundant in *Tnf*$^{-/-}$ lesions (Figure 4C, a versus b). The dLNs of *Tnf*$^{-/-}$ mice also contained more Arg1$^+$ cells and parasites than the respective WT organs, whereas the number of NOS2$^+$ cells was slightly reduced in *Tnf*$^{-/-}$ dLNs (Figures 4D, a versus b, and 4E; Figure S4A, c versus d).

NO is a precursor of peroxynitrite that causes tyrosine nitration of proteins and thereby acts as a footprint of NOS2 activity in tissues (Bogdan, 2015). Anti-nitrotyrosine staining of skin and dLN sections from *L. major*-infected WT mice yielded significantly stronger signals (number and MFI of positive cells) than in tissues from *Tnf*$^{-/-}$ mice (Figures 4C and 4D, c versus d, and 4F). Nitrotyrosine$^+$ cells stained positively for CD11b (Figures 4C and 4D, c versus d). In serial sections of *Tnf*$^{-/-}$ dLNs, expression of Arg1 by CD11b$^+$ cells correlated with a lack of nitrotyrosine staining despite the presence of NOS2 protein (Figure S4B). The nitrotyrosine staining was absent in tissue sections from naive C57BL/6 and infected *Nos2*$^{-/-}$ mice (Figures S4C, a versus b, and S4D) and after blocking of the anti-serum with 3-nitro-L-tyrosine (data not shown). To verify that the reduced nitrotyrosine staining in *Tnf*$^{-/-}$ mice reflects a lack of locally produced NO, we treated the sections with the NO-reactive compound 1,2-diaminoanthraquinone (DAQ). More NO was detected in infected dLNs of WT mice compared to dLNs of *Tnf*$^{-/-}$ mice (Figures 4G and S4E). Serial sections from infected *Nos2*$^{-/-}$ mice gave no signal with DAQ, despite the presence of CD11b$^+$ cells (Figure S4C, c versus d).

Together, these results show that Arg1 hyperexpression in *Tnf*$^{-/-}$ mice impairs the local production of NO and subsequently the control of *Leishmania* parasites.

Arg1 Expression Accounts for the Non-healing Course of *L. major* Infection

To test whether the increased Arg1 expression in *Tnf*$^{-/-}$ mice contributed to the detrimental course of *L. major* infection, we treated *L. major*-infected C57BL/6 WT or *Tnf*$^{-/-}$ mice with N$^{\omega}$-hydroxy-nor-L-arginine (nor-NOHA). Nor-NOHA, an arginine inhibitor that is neither tissue nor isoform selective (because it also blocks the arginine 2 isoform) (Custot et al., 1997), did not impede the arginase of *L. major* (Kropf et al., 2005) (data not

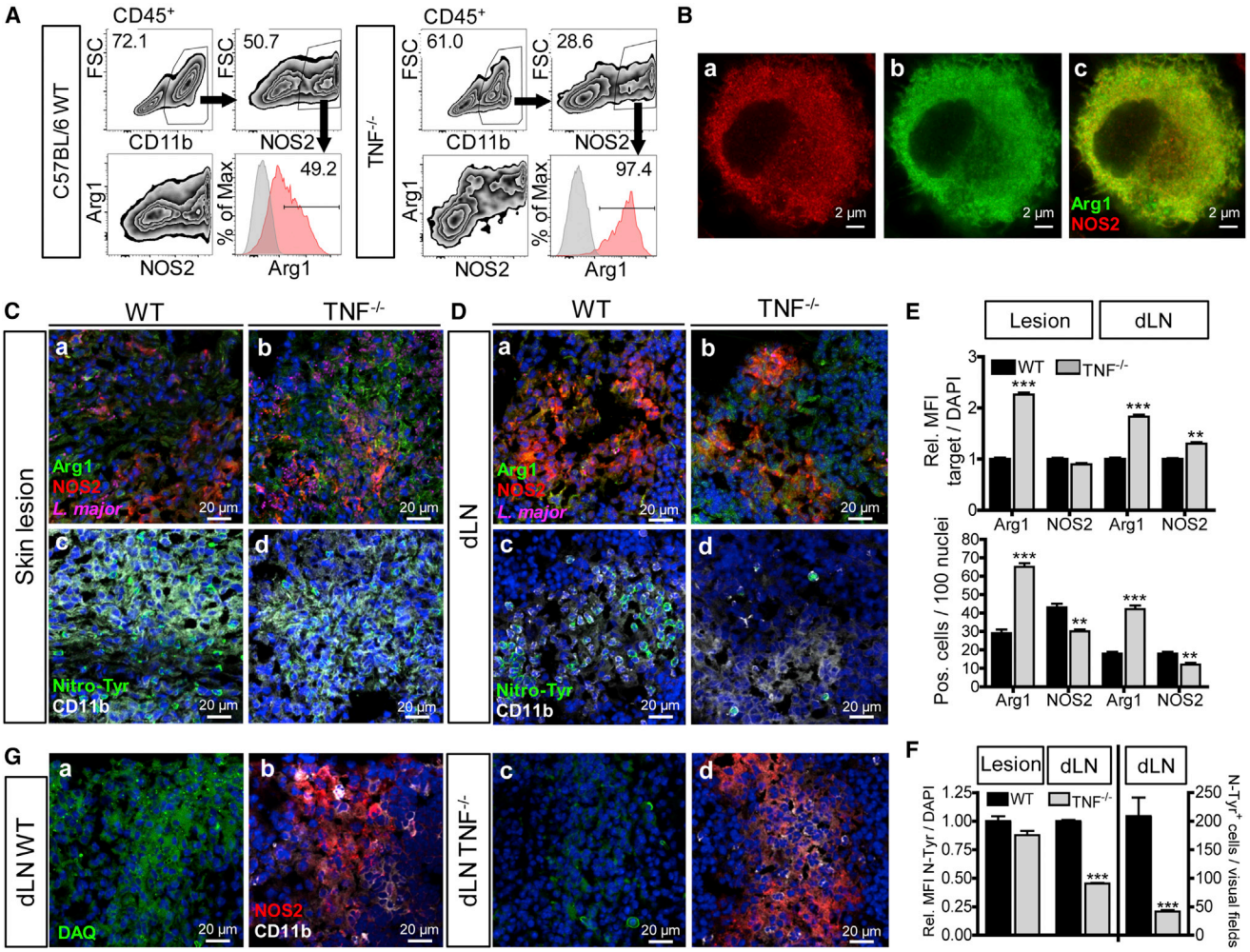

Figure 4. Increased Frequency of Arg1$^+$NOS2$^+$ Myeloid Cells Correlates with Decreased Detection of Nitrotyrosine and NO in *Tnf*$^{-/-}$ Mice

(A and C–G) C57BL/6 WT and *Tnf*$^{-/-}$ mice were infected with *L. major*. (A) Flow cytometry of skin lesions (23–29 dpi). NOS2$^+$ cells within viable CD11b$^+$CD45$^+$ single cells were gated and analyzed for co-expression of Arg1. The percentage of Arg1$^+$NOS2$^+$ cells within the NOS2$^+$ population was determined. One of three experiments.

(B) BMMs were stimulated with IL-4 (10 ng/ml) or IFN-γ (20 ng/ml) plus LPS (200 ng/ml) for 24 hr. Co-localization of Arg1 and NOS2 was analyzed by super-resolution microscopy. One of five experiments.

(C and D) Serial sections from skin lesions (C) or dLNs (D) at 26 dpi were stained for Arg1 (green), NOS2 (red), and *L. major* (magenta) (a and b) or for nitrotyrosine (green) and CD11b (white) (c and d). Nuclei staining with DAPI (blue). Due to marked differences in signal strength, exposure times had to be reduced for Arg1 (green) in skin sections of *Tnf*$^{-/-}$ mice. Representative images from one of four experiments, with three or four mice per group and time point (19–29 dpi).

(E and F) Quantification of the number and mean fluorescence intensity (MFI) of Arg1- or NOS2-positive cells (E) or nitrotyrosine-positive cells (F) in tissue sections of WT versus *Tnf*$^{-/-}$ mice (19–29 dpi). The target MFI was normalized to the fluorescence signal of DAPI. The number of positive cells was determined per 100 nuclei. Three or four visual fields (×200) per tissue section were evaluated. Analysis was of 17 dLNs and lesions of WT and *Tnf*$^{-/-}$ mice from four experiments.

(G) CLSFM of serial sections of dLNs from WT versus *Tnf*$^{-/-}$ mice stained for NO using DAQ (green) (a and c) or for NOS2 (red) and CD11b (white) (b and d). Representative images of four experiments, with three or four mice per group and time point (18–34 dpi).

**p < 0.01; ***p < 0.0001, two-tailed Mann-Whitney U test. See also Figures S3 and S4.

shown) but was reported to ameliorate the severity of *L. major* skin lesions in BALB/c mice (Iniesta et al., 2005; Kropf et al., 2005). Although in our hands this compound potently blocked Arg1 in macrophages in vitro (El-Gayar et al., 2003), the clinical course of *L. major* infection and the parasite loads in nor-NOHA-treated C57BL/6 WT or *Tnf*$^{-/-}$ mice were indistinguishable from the respective controls (data not shown). Furthermore, when testing nor-NOHA in *L. major*-infected BALB/c mice, neither local nor systemic application led to consistent protective effects (data not shown). We therefore abandoned the pharmacological approach and resorted to a model of cell-type-specific deletion of the *Arg1* gene using *Tie2cre*$^{+/-}$*Arg1*$^{fl/fl}$ mice (El Kasmi et al., 2008). The *Tie2cre* deleter is active in hematopoietic and endothelial cells. However, because Arg1 expression in *L. major*-infected mice was confined to CD45$^+$ cells (Figure S3B) identified as myeloid cells (Figure 3F),

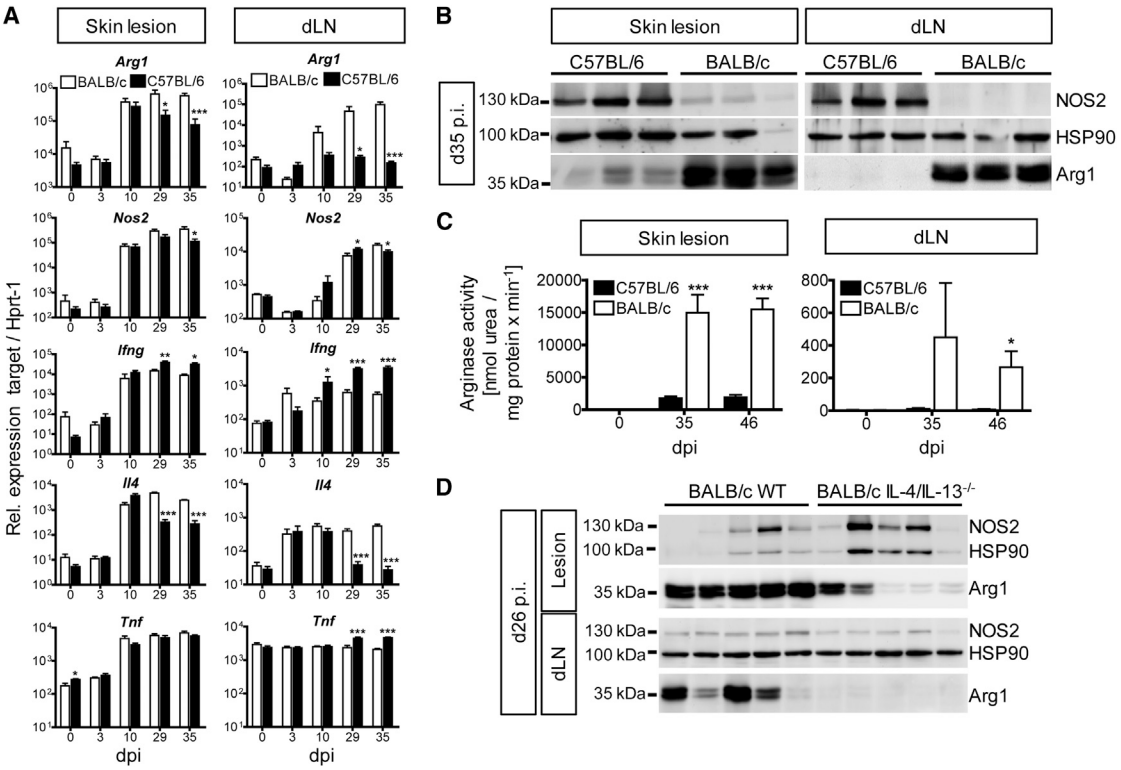

Figure 5. *L. major*-Infected BALB/c Mice Express Increased Levels of Arg1 in the Skin Lesions and dLNs Compared to Self-healing C57BL/6 Mice

BALB/c versus C57BL/6 or BALB/c WT versus *Il4/Il13*$^{-/-}$ mice were infected with *L. major*. Skin lesions and dLN tissue were analyzed at the time points indicated.

(A) A qRT-PCR analysis (means ± SEM from two experiments, with six mice per group and time point).

(B) Western blot analysis. One of four experiments.

(C) Arginase activity in protein lysates of skin lesions and dLNs (means ± SEM from two or three experiments, with three mice per group and time point).

(D) Western blot analysis. One of two experiments.

*p < 0.05; **p < 0.01; ***p < 0.005, two-tailed Mann-Whitney U test. See also Figures S5 and S6.

Tie2cre$^{+/-}$*Arg1*$^{fl/fl}$ mice are an efficient means of achieving myeloid-specific deletion of *Arg1* (Duque-Correa et al., 2014).

Tie2cre$^{+/-}$*Arg1*$^{fl/fl}$ mice were backcrossed to BALB/c. We chose the BALB/c background because similar to C57BL/6 *Tnf*$^{-/-}$ mice (Figure S2A), BALB/c WT mice developed progressive disease after *L. major* infection (Figure S5A). The amounts of Arg1 mRNA, protein, and activity in the skin lesions (Iniesta et al., 2005; Kropf et al., 2005) and dLNs of *L. major*-infected BALB/c mice were higher than in self-healing C57BL/6 mice (Figures 5A–5C, S5B, and S5C). In both strains of mice, Arg1 was more prominent in the skin than in dLNs, which is in line with the differential expression of IL-4 at these two sites (Figure 5A). Despite comparable quantities of *Nos2* mRNA in BALB/c and C57BL/6 mice (Figure 5A), NOS2 protein was markedly reduced in *L. major*-infected BALB/c mice (Figure 5B). The reciprocal expression of Arg1 and NOS2 protein suggests that the translational control of NOS2 by Arg1 activity observed in vitro (El-Gayar et al., 2003) also occurs in vivo.

In BALB/c mice, the increased amounts of Arg1 were accompanied by persistent *Il4* mRNA and reduced levels of *Ifng* and *Tnf* mRNA (Figure 5A). To test whether the Th2 cytokine milieu and Arg1 hyperexpression were causally linked, we used *Il4*$^{-/-}$ or IL-4/IL-13-double-deficient BALB/c mice. Unlike BALB/c WT mice, both *Il4*$^{-/-}$ and *Il4/Il13*$^{-/-}$ mice contained the infection (Figures S5D and S5G) and showed a strong reduction (lesions) or abolition (dLNs) of Arg1 mRNA and protein expression (Figures 5D, S5E, S5F, and S5H–S5J). The residual amount of Arg1 in the skin lesions of *Il4/Il13*$^{-/-}$ mice might reflect the activity of other Arg1-inducing cytokines or of microbial ligands. The Arg1^{+} myeloid cell population in skin lesions of *L. major*-infected BALB/c WT mice showed the same surface phenotype (i.e., CD11b^{+}CD11c^{+}MHCII^{+}Ly6C^{+}CD64^{+}PDL2^{+}CD207^{-}CCR7^{-}) (Figure S6), as seen in C57BL/6 WT and *Tnf*$^{-/-}$ mice.

As expected, Arg1-expressing *Tie2cre*$^{-/-}$*Arg1*$^{fl/fl}$ or *Tie2cre*$^{+/-}$*Arg1*$^{wt/wt}$ BALB/c mice developed ulcerative skin lesions and visceral disease following *L. major* infection. In contrast, the Arg1-deficient *Tie2cre*$^{+/-}$*Arg1*$^{fl/fl}$ littermates presented only small, non-ulcerative and non-progressive skin swellings after low (1×10^4) infection inocula (data not shown) or high (3×10^6) infection inocula (Figure 6A) and showed a significantly reduced parasite burden at the site of infection, in the dLNs, and in the spleen (Figure 6B). No spontaneous reactivation of disease in *Tie2cre*$^{+/-}$*Arg1*$^{fl/fl}$ BALB/c mice occurred during the observation period (≤274 days) (Figure 6C). The

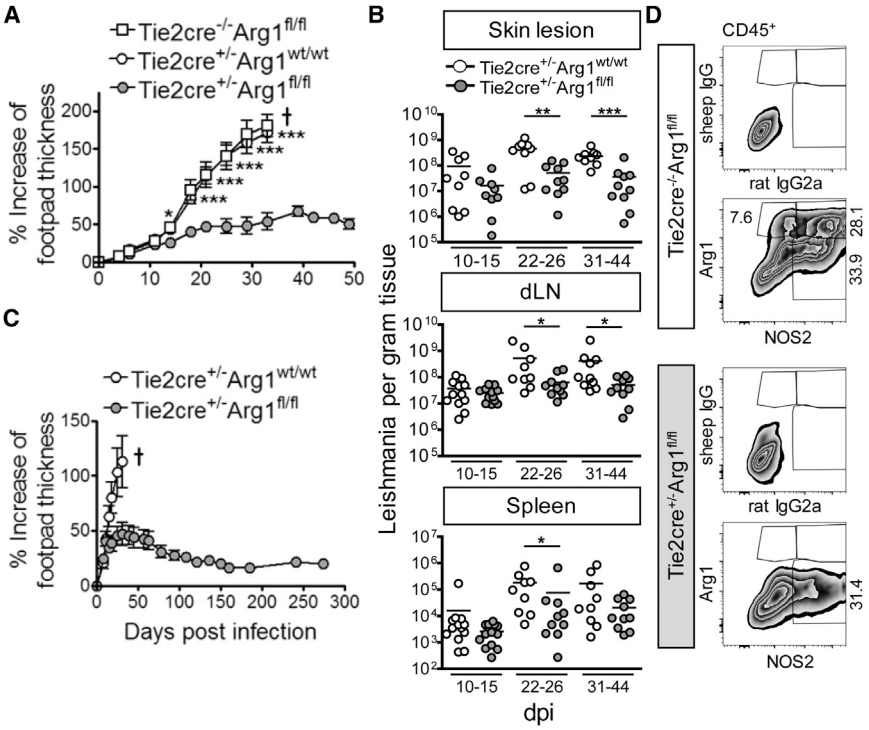

Figure 6. Arg1-Deficient BALB/c Mice Are Protected from Progressive Cutaneous Leishmaniasis

Arg1-deficient BALB/c mice (*Tie2cre*$^{+/-}$*Arg1*$^{fl/fl}$) and control littermates (*Tie2cre*$^{+/-}$*Arg1*$^{wt/wt}$ or *Tie2cre*$^{-/-}$*Arg1*$^{fl/fl}$) were infected with *L. major*.

(A and C) Clinical course of infection. Six to nine (A) or four to six (C) mice were used per group (means ± SEM). One of six (A) or two (C) experiments. †, mice had to be euthanized for ethical reasons.

(B) Parasite numbers in the tissues (results represent the mean of 9–12 mice that were analyzed in three or four experiments, with 3 mice per group and time point).

(D) Flow cytometry of skin lesions (23 dpi). Cells were gated on viable single CD45$^+$ cells (Figure S3A), and the percentage of Arg1$^+$, NOS2$^+$, or Arg1$^+$NOS2$^+$ cells was determined using the respective isotype controls. One of two experiments.

*$p < 0.05$; **$p < 0.01$; ***$p < 0.005$, two-tailed Mann-Whitney U test. See also Figures S7A and S7B.

efficiency of deletion of Arg1 expression was >99.5% (Figures 6D, S7A, and S7B).

Analyses of infected tissues revealed a slight but significant reduction of *Il10* mRNA in the dLNs from Arg1-deficient *Tie2cre*$^{+/-}$*Arg1*$^{fl/fl}$ BALB/c mice, whereas *Ifng* and *Il4* mRNAs remained unaltered (Figure 7A). Considering that Arg1 activity can diminish the availability of L-arginine and thereby might affect T cell differentiation and/or proliferation (Bogdan, 2015; Duque-Correa et al., 2014; Munder et al., 2009; Pesce et al., 2009), we studied the T cell response in *L. major*-infected *Tie2cre*$^{-/-}$*Arg1*$^{fl/fl}$ BALB/c versus *Tie2cre*$^{+/-}$*Arg1*$^{fl/fl}$ BALB/c mice. First, CD4$^+$CD3$^+$ T cells of dLNs from both mouse strains were analyzed for their expression of the transcription factors T-bet (Th1), GATA3 (Th2), and RORγt (Th17) to evaluate the expansion of T helper cell subsets. Whereas T-bet$^+$ or RORγt$^+$ CD4$^+$ T cells were hardly detectable, the high percentage of GATA3$^+$ T cells in both WT and Arg1-deficient dLNs demonstrated a sustained Th2 response (Figure 7B). Despite a significantly reduced (~30%) frequency of CD4$^+$GATA3$^+$ T cells at later time points of infection in the Arg1-deficient BALB/c mice, the *Il4* mRNA expression was altered in neither whole dLNs (Figure 7A) nor sorted CD4$^+$CD3$^+$ dLN cells (Figure 7C). Thus, the net response of Th2 effector cells was not reduced in Arg1-deficient BALB/c mice. Second, the expression of *Ifng*, *Il10*, and *Il17a* or *Il17f* mRNA was comparable in CD4$^+$ or CD8$^+$ T cells sorted from both groups of mice (Figure 7C). Third, there was no difference in the percentage of Foxp3$^+$CD4$^+$ regulatory T (Treg) cells in the dLNs at different time points of infection (Figure 7D). Finally, when we measured the proliferative capacity of CD4$^+$ or CD8$^+$ T cells in vivo using bromodeoxyuridine (BrdU) incorporation, absence of Arg1 was associated with either unaltered (two experiments) or slightly reduced (one experiment) but not with improved T cell proliferation (Figure 7E).

The deletion of *Arg1* did not lead to up-regulation of *Nos2* mRNA or protein at the site of infection or in the dLNs; the qRT-PCR analyses and the western blot experiments even revealed slightly diminished *Nos2* mRNA and protein expression in Arg1-deficient mice (Figures 7A, 7F, and S7A). Nevertheless, Arg1 deficiency caused a marked increase of nitrotyrosine-positive cells and of the production of NO (as detected by DAQ) in the skin lesions and dLNs (Figure 7G, S7C, and S7D).

Taken together, these data allow us to conclude that hyperexpression of Arg1, as seen in non-healing BALB/c or C57BL/6 *Tnf*$^{-/-}$ mice, does not deviate the T cell response against *L. major* but markedly impairs the in situ generation of protective NO and thereby interferes with disease control.

DISCUSSION

TNF as Regulator of Immune Responses

TNF is best known for its potent proinflammatory effects resulting from its ability to promote the proliferation or enhance the function of macrophages, dendritic cells, B lymphocytes, T lymphocytes, natural killer cells, and other types of immune cells (Vassalli, 1992). While this immunostimulatory function of TNF confers protection of the host organism against infectious pathogens (Flynn et al., 1995; Grivennikov et al., 2005; Körner et al., 2010; Marino et al., 1997; Novosad and Winthrop, 2014; Pfeffer et al., 1993; Vassalli, 1992), overproduction of TNF is a typical feature of autoimmune and other chronic inflammatory diseases, leading to tissue destruction in mice and humans (Atreya et al., 2014; Riminton et al., 1998; Vassalli, 1992). Previous studies showed that TNF can mediate control of intracellular infections by the stimulation of the anti-microbial activity of phagocytes (Bogdan, 2015; Yazdanpanah et al., 2009); the activation of

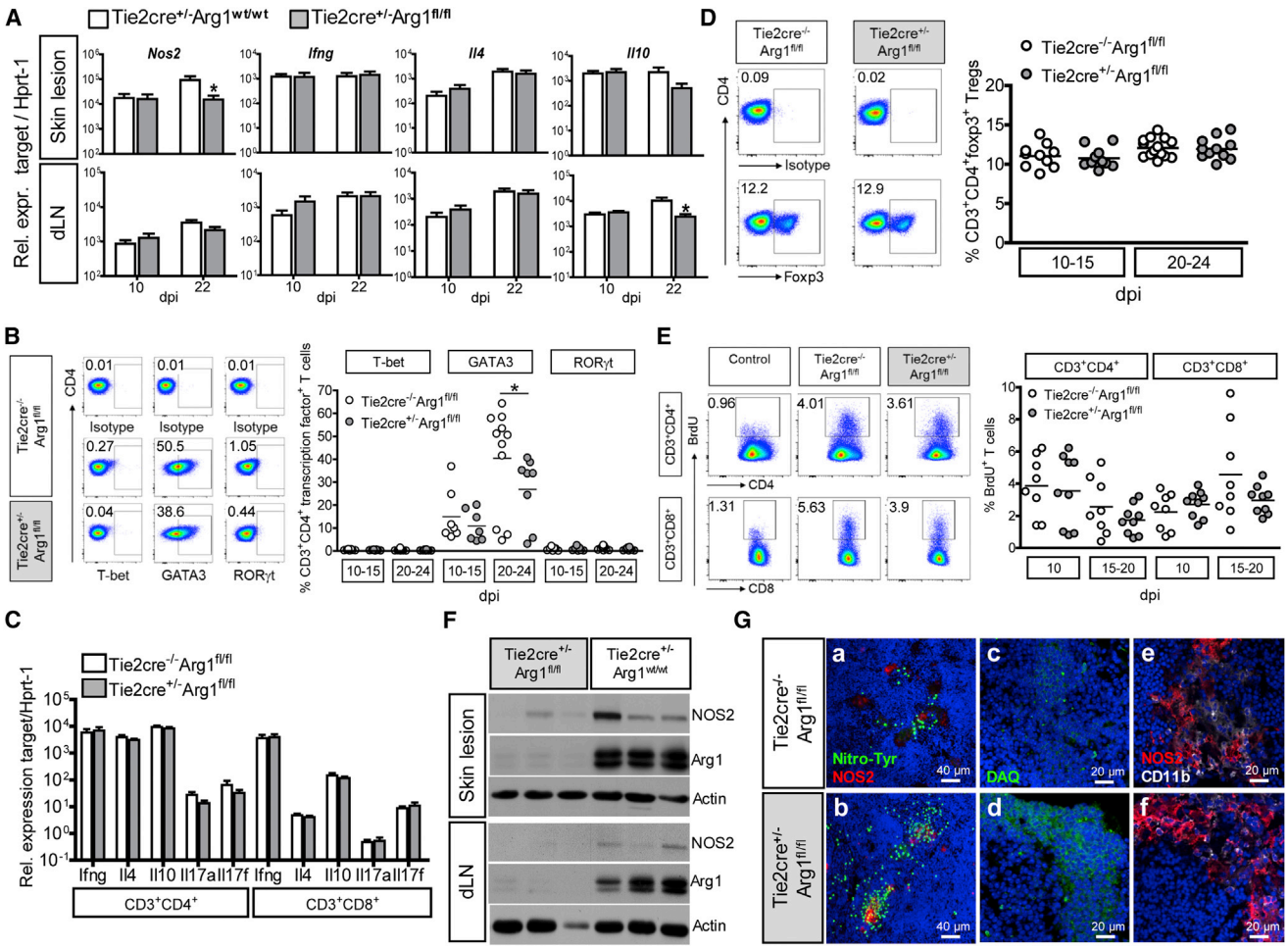

Figure 7. Increased NO Production but Unaltered T Cell Response in Arg1-Deficient BALB/c Mice

Arg1-deficient BALB/c mice (*Tie2cre*$^{+/-}$*Arg1*$^{fl/fl}$) and control littermates (*Tie2cre*$^{+/-}$*Arg1*$^{wt/wt}$ or *Tie2cre*$^{-/-}$*Arg1*$^{fl/fl}$) were infected with *L. major*.

(A) A qRT-PCR analysis (means ± SEM of three experiments, with three or four mice per group and time point).

(B) The dLN cells (stained for CD3, CD4, CD8, and NKp46 and T-bet, GATA3, or RORγt) were gated on viable CD3$^+$CD4$^+$CD8$^-$Nkp46$^-$ cells, and the percentage of T-bet-, GATA3-, or RORγt-positive cells was determined. Representative dot plots and means of three experiments, with two to four mice per group and time point.

(C) A qRT-PCR analysis of CD3$^+$CD4$^+$ and CD3$^+$CD8$^+$ T cells sorted from the dLNs of infected mice (three per group) at 17–22 dpi. Means ± SEM of three experiments.

(D) The dLN cells (stained for CD3, CD4, CD8, and Foxp3) were gated on viable CD3$^+$CD4$^+$CD8$^-$ T cells, and the percentage of Foxp3$^+$ Treg cells was determined. Representative dot plots and means of four experiments, with two to four mice per group and time point.

(E) The dLN cells from BrdU-injected mice were stained for CD3, CD4, CD8, and BrdU. BrdU$^+$ cells (excluding doublets and dead cells) within the CD3$^+$CD4$^+$ or CD3$^+$CD8$^+$ T cell population were gated. Representative dot plots and means of three experiments, with three mice per group and time point. The dLN cells from infected WT mice without BrdU treatment were used as controls for the BrdU staining.

(F) Western blot analysis of skin lesions and dLNs (18 dpi). One of five experiments, with three or four mice per group and time point.

(G) CLSFM analysis of dLNs that were stained for nitrotyrosine (green) and NOS2 (red) (a and b) and in serial sections for NO (c and d) visualized by DAQ (green) and for NOS2 (red) and CD11b (white) (e and f). Nuclei were stained with DAPI (blue). Representative images from three experiments, with four mice per group and time point analyzed at 17–32 dpi.

*p < 0.05, two-tailed Mann-Whitney U test. See also Figures S7C and S7D.

T helper cells or cytotoxic T cells (Vassalli, 1992); the differentiation, functional maturation, or survival of myeloid cells (Caux et al., 1992; Fromm et al., 2012; Sade-Feldman et al., 2013); and the generation of non-necrotizing granulomas (Flynn et al., 1995; Marino et al., 1997).

Our present work revealed that TNF downregulated Arg1 in vitro and in vivo and thereby unleashed the enzymatic activity of NOS2 and the production of NO. TNF also antagonized other aspects of macrophage activation by IL-4, including the IL-4-induced oxidative metabolism. TNF did not inhibit the phosphorylation or nuclear translocation of STAT6 but suppressed IL-4-triggered histone acetylation of the *Arg1* promoter and putative regulatory or enhancer regions, which is likely to impede access or binding of STAT6 to these sites and/or its assembly

with other relevant transcription factors (e.g., C/EBPβ) (Pauleau et al., 2004; Sheldon et al., 2013). We currently investigate whether TNF regulates histone acetyl-transferases or deacetylases, which are critical for the induction of Arg1 by IL-4 (Serrat et al., 2012). Hyperexpression of Arg1, resulting from the failure to shut down IL-4 or the lack of TNF, presumably accounts for the exquisite *L. major* susceptibility of BALB/c or $Tnf^{-/-}$ mice, respectively, because deletion of *Arg1* alone was sufficient to restore local NO production and to prevent non-healing disease in BALB/c mice. Furthermore, we defined inflammatory monocyte-derived dendritic cells or macrophages as the principle source of Arg1 at the infection site. The high rate of intracellular co-expression of Arg1 and NOS2 seen by high-resolution microscopy in IL-4/IFN-γ/LPS-stimulated macrophages in vitro and in infected $Tnf^{-/-}$ mice facilitated the ability of Arg1 to effectively impair the production of NO in situ.

Earlier studies reported upregulation of Arg1 by TNF in endothelial cells in a model of coronary ischemia and reperfusion injury (Gao et al., 2007) or in myeloid suppressor cells during chronic inflammation elicited by repeated subcutaneous injections of heat-killed *Mycobacterium bovis* Bacille Calmette Guerin (Sade-Feldman et al., 2013). While these experimental settings were entirely different from the infection model used here, our results do not exclude a divergent role of TNF during infections with other pathogens or in other organs.

Arginase and Pathogen Control

Arg1 expression might impair anti-microbial defense in vivo by three mechanisms (Bogdan, 2015): (1) Arg1 can deplete myeloid cells of L-arginine, thereby impeding the generation of NO by NOS2; (2) Arg1 of myeloid cells is capable of depriving T lymphocytes of L-arginine, which was reported to decrease their proliferation, survival, and/or expression of costimulatory molecules in vitro; and (3) Arg1 activity leads to the generation of ornithine and via the ornithine decarboxylase (ODC) pathway to the synthesis of polyamines, which are essential for the growth of various parasites, including *Leishmania* (Colotti and Ilari, 2011). However, as *L. major* expresses its own arginase and ODC (Reguera et al., 2009), its survival is unlikely to be affected by exogenous polyamines derived from host cells. With respect to the second possible mechanism of Arg1 action, we avoided the use of in vitro culture systems, which are prone to distort the true proliferative capacity of T cells due to the high L-arginine content of the culture media. Instead, we studied the differentiation and proliferation of $CD4^+$ or $CD8^+$ T cells in vivo using $Tie2cre^{-/-}Arg1^{fl/fl}$ or $Tie2cre^{+/-}Arg1^{fl/fl}$ mice. These analyses revealed an unaltered proliferation of T cells in situ without any apparent shift in the T helper cell differentiation, the abundance of Treg cells, or the expression of T helper cell cytokines, irrespective of the presence or absence of Arg1. In contrast, the generation of NO by NOS2 was severely impaired when Arg1 was hyperexpressed. Thus, our data clearly show that the counterprotective function of Arg1 primarily results from its competition with NOS2.

TNF and Leishmaniasis

Previous studies emphasized the role of TNF as a co-activator of macrophages for the expression of NOS2 activity. Exogenous or endogenous TNF clearly synergized with IFN-γ for the induction of NOS2/NO in inflammatory macrophages in vitro (Wilhelm et al., 2001) and in vivo (Olekhnovitch et al., 2014) and for the killing of intracellular *Leishmania* parasites (Green et al., 1990; Liew et al., 1990). At least in BMMs, TNF might induce NOS2 even on its own, as shown in the present study (Figures 1A and 1F). So far, it has been assumed that the remarkable susceptibility to *L. major* seen in mice lacking TNF (Allenbach et al., 2008; Titus et al., 1989; Wilhelm et al., 2001) results from impaired macrophage activation. However, TNFR1/TNFR2 double-deficient mice (Nashleanas et al., 1998) and $Tnf^{-/-}$ mice (Wilhelm et al., 2001; De Trez et al., 2009) maintained the expression of *Nos2* mRNA and protein in the dLNs, and *L. major*-infected macrophages from these mice were still capable of expressing NOS2 and killing intracellular parasites in response to IFN-γ (Nashleanas et al., 1998). These findings already indicated that the synergism with IFN-γ might not be the only or leading mechanism of action of TNF in vivo.

Our study demonstrates that TNF suppresses the IL-4-dependent expression of Arg1 in myeloid cells and thereby generates a micromilieu that allows for enhanced generation of NO by NOS2 in situ and improved parasite control. It will be of interest to assess whether TNF functions in the same way in patients with autoimmune diseases, who have an increased risk to develop severe infections with *Leishmania* or other intracellular pathogens following anti-TNF treatment (Novosad and Winthrop, 2014; Tung Chen et al., 2014). The observations that TNF signaling antagonized M2 gene expression in spinal cord injury (Kroner et al., 2014) and in solid tumors (Kratochvill et al., 2015) and that two other TNF superfamily members (BAFF and APRIL) caused downregulation of M2 markers (Allman et al., 2015) suggest that the suppression of Arg1 by TNF and TNF-related molecules forms a general paradigm in immunology. Considering that Arg1-expressing myeloid cells contribute to the pathogenesis of numerous diseases, ranging from chronic infections to malignant tumors and progressive organ fibrosis, our findings have implications for novel treatment strategies and call for caution when using TNF-neutralizing agents.

EXPERIMENTAL PROCEDURES

Mouse Strains

C57BL/6 or BALB/c WT or transgenic mice (C57BL/6 $Tnf^{-/-}$, C57BL/6 $Nos2^{-/-}$, BALB/c $Il4^{-/-}$, BALB/c $Il4/Il13^{-/-}$, conditional Arg1-deficient BALB/c or C57BL/6 mice [$Tie2Cre^{+/-}Arg1^{fl/fl}$ versus $Tie2Cre^{+/-}Arg1^{wt/wt}$ or $Tie2Cre^{-/-}Arg1^{fl/fl}$]) were used at 8–14 weeks of age. Infections were performed with female mice and the respective age-matched WT or littermate controls. Mice were kept under SPF conditions. Animal care and experiments were conducted in accordance with German regulations after local governmental approval (Freiburg, Ansbach and Würzburg, Germany).

Infection and In Vivo Treatment of Mice

Mice were infected bilaterally into the skin of the hindfoot with 3×10^6 stationary-phase *L. major* promastigotes (strain MHOM/IL/81/FEBNI) in 50 μl PBS. The clinical monitoring of the infection by measuring the footpad thickness, the determination of the parasite burden by limiting dilution analyses, and the applications of drugs are described in the Supplemental Experimental Procedures.

Cell Culture and Measurements of Cellular Activities

BMDCs and BMMs were generated from bone marrow cells (Prajeeth et al., 2011) and used at day 7 or 8 to day 10 of culture, respectively. Then,

recombinant mouse interleukin-4 (0.5–10 ng/ml) and recombinant mouse tumor necrosis factor (10 or 50 ng/ml) (R&D Systems) were added as the stimulant or stimulants. At the concentrations used, the LPS content of all reagents and the supplemented media was ≤10 pg/ml (colorimetric *Limulus* amebocyte lysate assay, Whittaker M.A. Bioproducts).

The composition of the culture media and the determination of nitrite, arginase activity, and energy metabolism (OCR and ECAR) are described in the Supplemental Experimental Procedures.

qPCR

Total RNA was extracted from homogenized tissue or cultured cells using the TRIfast reagent (Peqlab). Then, 1–5 μg RNA were reverse transcribed using the High-Capacity cDNA Archive Kit (Thermo Fisher Scientific). Next, qPCR was performed on the ABI7900HT Fast Real Time PCR system (Applied Biosystems; Thermo Fisher Scientific). For the gene-specific assays used, see the Supplemental Experimental Procedures. The mRNA levels were calculated using the following formula: relative expression = $2^{-(C_{T(Target)} - C_{T(Endogenous\ control)})} \times f$, with $f = 10^4$ as an arbitrary factor. In some experiments, relative expression was calibrated to controls, as indicated in the legends.

ChIP

ChIP was performed as described (Garber et al., 2012; Ostuni et al., 2013). In brief, nuclear extracts obtained from 12 × 10^6 fixed BMMs were sheared by sonication and incubated overnight at 4°C with protein G Dynabeads (Invitrogen), coupled with 2.5 μg of anti-H3K27ac antibody (ab4729, Abcam). After ChIP, beads were magnetically recovered and washed and DNA was eluted and decrosslinked overnight at 65°C. DNA was then purified with solid-phase reversible immobilization beads (Agencourt AMPure XP, Beckman Coulter) and quantified with PicoGreen (Invitrogen). For ChIP-qPCR experiments, 1 μl of purified DNA (immunoprecipitation and 1% input) was used for amplification on an ABI7500 machine. Primers are listed in the Supplemental Experimental Procedures.

Flow Cytometry

See the Supplemental Experimental Procedures.

Western Blot Analysis and Immunoprecipitations

See the Supplemental Experimental Procedures.

Immunohistology and Microscopy

See the Supplemental Experimental Procedures.

Statistical Analyses

Results are displayed as mean ± SEM and were statistically analyzed using GraphPad Prism v.4 or v.6, as detailed in the figure legends.

SUPPLEMENTAL INFORMATION

Supplemental Information includes Supplemental Experimental Procedures and seven figures and can be found with this article online at http://dx.doi.org/10.1016/j.celrep.2016.04.001.

AUTHOR CONTRIBUTIONS

U.S., H.K., R.O., and C.B. conceived and designed the experiments. U.S., K.P., A.D., R.O., S.O., D.M., T.K., J.C.K., and C.B. performed the experiments. U.S., K.P., A.D., T.K., J.C.K., D.M., H.K., and C.B. analyzed the data. E.R., D.D., and P.J.M. contributed reagents, materials, mouse strains, technical know-how, and ideas. C.B., U.S., K.P., P.J.M., and H.K. wrote the paper.

ACKNOWLEDGMENTS

The authors are grateful to Claudia Kurzmann, Rosa Mammato, and Heidi Sebald for excellent technical assistance during the starting phase of this project; to Katharina Pracht for participating in pilot experiments; and to Ralf Willebrand, Christian Schwartz, and Manfred Lutz for advice. We also thank Tristan Nowak and Ralf Palmisano from the Optimal Imaging Center Erlangen (OICE) of the FAU for help with the stimulated emission depletion microscopy, the operators of the Core Facility for Cell-Sorting and Immunomonitoring, and the personnel of the Franz-Penzoldt Animal Center Erlangen of the FAU for animal care. This study was supported by grants to C.B., U.S., and D.D. from the Deutsche Forschungsgemeinschaft (DFG-SFB620, A9; DFG-GRK1660, A5; DFG-SFB643, A6, A7; and DFG-SFB1181, C4, A7); to C.B. and U.S. from the Interdisciplinary Center for Clinical Research of the FAU (A24, A61); to C.B. from the Emerging Field Initiative of the FAU (Medicinal Inorganic Redox Chemistry consortium) and from the Dr. Robert Pfleger-Stiftung; to D.D. from the Bavarian Genome Network (BayGene); to P.J.M. from the NIH (CA189990, Cancer Center Core Grant P30 CA21765) and the American Lebanese Syrian Associated Charities of St. Jude Children's Research Hospital; and to H.K. from the National Health and Medical Research Council of Australia (NHMRC 485807).

Received: February 8, 2015
Revised: February 9, 2016
Accepted: March 25, 2016
Published: April 21, 2016

REFERENCES

Allenbach, C., Launois, P., Mueller, C., and Tacchini-Cottier, F. (2008). An essential role for transmembrane TNF in the resolution of the inflammatory lesion induced by *Leishmania major* infection. Eur. J. Immunol. *38*, 720–731.

Allman, W.R., Dey, R., Liu, L., Siddiqui, S., Coleman, A.S., Bhattacharya, P., Yano, M., Uslu, K., Takeda, K., Nakhasi, H.L., and Akkoyunlu, M. (2015). TACI deficiency leads to alternatively activated macrophage phenotype and susceptibility to *Leishmania* infection. Proc. Natl. Acad. Sci. USA *112*, E4094–E4103.

Atreya, R., Neumann, H., Neufert, C., Waldner, M.J., Billmeier, U., Zopf, Y., Willma, M., App, C., Münster, T., Kessler, H., et al. (2014). In vivo imaging using fluorescent antibodies to tumor necrosis factor predicts therapeutic response in Crohn's disease. Nat. Med. *20*, 313–318.

Bogdan, C. (2015). Nitric oxide synthase in innate and adaptive immunity: an update. Trends Immunol. *36*, 161–178.

Caux, C., Dezutter-Dambuyant, C., Schmitt, D., and Banchereau, J. (1992). GM-CSF and TNF-alpha cooperate in the generation of dendritic Langerhans cells. Nature *360*, 258–261.

Colegio, O.R., Chu, N.Q., Szabo, A.L., Chu, T., Rhebergen, A.M., Jairam, V., Cyrus, N., Brokowski, C.E., Eisenbarth, S.C., Phillips, G.M., et al. (2014). Functional polarization of tumour-associated macrophages by tumour-derived lactic acid. Nature *513*, 559–563.

Colotti, G., and Ilari, A. (2011). Polyamine metabolism in *Leishmania*: from arginine to trypanothione. Amino Acids *40*, 269–285.

Creyghton, M.P., Cheng, A.W., Welstead, G.G., Kooistra, T., Carey, B.W., Steine, E.J., Hanna, J., Lodato, M.A., Frampton, G.M., Sharp, P.A., et al. (2010). Histone H3K27ac separates active from poised enhancers and predicts developmental state. Proc. Natl. Acad. Sci. USA *107*, 21931–21936.

Custot, J., Moali, C., Brollo, M., Boucher, J.L., Delaforge, M., Mansuy, D., Tenu, J.P., and Zimmermann, J.L. (1997). The new α-amino acid N^{ω}-hydroxy-nor-L-arginine: a high-affinity inhibitor of arginase well adapted to bind to its manganese cluster. J. Am. Chem. Soc. *119*, 4086–4087.

De Muylder, G., Daulouède, S., Lecordier, L., Uzureau, P., Morias, Y., Van Den Abbeele, J., Caljon, G., Hérin, M., Holzmuller, P., Semballa, S., et al. (2013). A *Trypanosoma brucei* kinesin heavy chain promotes parasite growth by triggering host arginase activity. PLoS Pathog. *9*, e1003731.

De Trez, C., Magez, S., Akira, S., Ryffel, B., Carlier, Y., and Mraille, E. (2009). iNOS-producing inflammatory dendritic cells constitute the major infected cell type during the chronic *Leishmania major* infection of C57BL/6 resistant mice. PLoS Pathogens *5*, e1000494.

Diefenbach, A., Schindler, H., Donhauser, N., Lorenz, E., Laskay, T., MacMicking, J., Röllinghoff, M., Gresser, I., and Bogdan, C. (1998). Type 1 interferon

(IFNalpha/beta) and type 2 nitric oxide synthase regulate the innate immune response to a protozoan parasite. Immunity *8*, 77–87.

Duque-Correa, M.A., Kühl, A.A., Rodriguez, P.C., Zedler, U., Schommer-Leitner, S., Rao, M., Weiner, J., 3rd, Hurwitz, R., Qualls, J.E., Kosmiadi, G.A., et al. (2014). Macrophage arginase-1 controls bacterial growth and pathology in hypoxic tuberculosis granulomas. Proc. Natl. Acad. Sci. USA *111*, E4024–E4032.

El-Gayar, S., Thüring-Nahler, H., Pfeilschifter, J., Röllinghoff, M., and Bogdan, C. (2003). Translational control of inducible nitric oxide synthase by IL-13 and arginine availability in inflammatory macrophages. J. Immunol. *171*, 4561–4568.

El Kasmi, K.C., Qualls, J.E., PesFce, J.T., Smith, A.M., Thompson, R.W., Henao-Tamayo, M., Basaraba, R.J., König, T., Schleicher, U., Koo, M.S., et al. (2008). Toll-like receptor-induced arginase 1 in macrophages thwarts effective immunity against intracellular pathogens. Nat. Immunol. *9*, 1399–1406.

Flynn, J.L., Goldstein, M.M., Chan, J., Triebold, K.J., Pfeffer, K., Lowenstein, C.J., Schreiber, R., Mak, T.W., and Bloom, B.R. (1995). Tumor necrosis factor-alpha is required in the protective immune response against *Mycobacterium tuberculosis* in mice. Immunity *2*, 561–572.

Fromm, P.D., Kling, J., Mack, M., Sedgwick, J.D., and Körner, H. (2012). Loss of TNF signaling facilitates the development of a novel Ly-6C(low) macrophage population permissive for *Leishmania major* infection. J. Immunol. *188*, 6258–6266.

Gao, X., Xu, X., Belmadani, S., Park, Y., Tang, Z., Feldman, A.M., Chilian, W.M., and Zhang, C. (2007). TNF-alpha contributes to endothelial dysfunction by upregulating arginase in ischemia/reperfusion injury. Arterioscler. Thromb. Vasc. Biol. *27*, 1269–1275.

Garber, M., Yosef, N., Goren, A., Raychowdhury, R., Thielke, A., Guttman, M., Robinson, J., Minie, B., Chevrier, N., Itzhaki, Z., et al. (2012). A high-throughput chromatin immunoprecipitation approach reveals principles of dynamic gene regulation in mammals. Mol. Cell *47*, 810–822.

Gautier, E.L., Shay, T., Miller, J., Greter, M., Jakubzick, C., Ivanov, S., Helft, J., Chow, A., Elpek, K.G., Gordonov, S., et al.; Immunological Genome Consortium (2012). Gene-expression profiles and transcriptional regulatory pathways that underlie the identity and diversity of mouse tissue macrophages. Nat. Immunol. *13*, 1118–1128.

Ginhoux, F., Schultze, J.L., Murray, P.J., Ochando, J., and Biswas, S.K. (2015). New insights into the multidimensional concept of macrophage ontogeny, activation and function. Nat. Immunol. *17*, 34–40.

Green, S.J., Crawford, R.M., Hockmeyer, J.T., Meltzer, M.S., and Nacy, C.A. (1990). *Leishmania major* amastigotes initiate the L-arginine-dependent killing mechanism in IFN-γ-stimulated macrophages by induction of tumor necrosis factor-α. J. Immunol. *145*, 4290–4297.

Grivennikov, S.I., Tumanov, A.V., Liepinsh, D.J., Kruglov, A.A., Marakusha, B.I., Shakhov, A.N., Murakami, T., Drutskaya, L.N., Förster, I., Clausen, B.E., et al. (2005). Distinct and nonredundant in vivo functions of TNF produced by t cells and macrophages/neutrophils: protective and deleterious effects. Immunity *22*, 93–104.

Huang, S.C., Everts, B., Ivanova, Y., O'Sullivan, D., Nascimento, M., Smith, A.M., Beatty, W., Love-Gregory, L., Lam, W.Y., O'Neill, C.M., et al. (2014). Cell-intrinsic lysosomal lipolysis is essential for alternative activation of macrophages. Nat. Immunol. *15*, 846–855.

Iniesta, V., Carcelén, J., Molano, I., Peixoto, P.M.V., Redondo, E., Parra, P., Mangas, M., Monroy, I., Campo, M.L., Nieto, C.G., and Corraliza, I. (2005). Arginase I induction during *Leishmania major* infection mediates the development of disease. Infect. Immun. *73*, 6085–6090.

Iyer, R.K., Yoo, P.K., Kern, R.M., Rozengurt, N., Tsoa, R., O'Brien, W.E., Yu, H., Grody, W.W., and Cederbaum, S.D. (2002). Mouse model for human arginase deficiency. Mol. Cell. Biol. *22*, 4491–4498.

Kirchner, H., Holden, H.T., and Herberman. (1975). Splenic suppressor macrophages induced in mice by injection of *Corynebacterium parvum*. J. Immunol. *115*, 1212–1216.

Körner, H., McMorran, B., Schlüter, D., and Fromm, P. (2010). The role of TNF in parasitic diseases: still more questions than answers. Int. J. Parasitol. *40*, 879–888.

Kratochvill, F., Neale, G., Haverkamp, J.M., Van de Velde, L.A., Smith, A.M., Kawauchi, D., McEvoy, J., Roussel, M.F., Dyer, M.A., Qualls, J.E., and Murray, P.J. (2015). TNF counterbalances the emergence of M2 tumor macrophages. Cell Rep. *12*, 1902–1914.

Kroner, A., Greenhalgh, A.D., Zarruk, J.G., Passos Dos Santos, R., Gaestel, M., and David, S. (2014). TNF and increased intracellular iron alter macrophage polarization to a detrimental M1 phenotype in the injured spinal cord. Neuron *83*, 1098–1116.

Kropf, P., Fuentes, J.M., Fähnrich, E., Arpa, L., Herath, S., Weber, V., Soler, G., Celada, A., Modolell, M., and Müller, I. (2005). Arginase and polyamine synthesis are key factors in the regulation of experimental leishmaniasis in vivo. FASEB J. *19*, 1000–1002.

Lavin, Y., Winter, D., Blecher-Gonen, R., David, E., Keren-Shaul, H., Merad, M., Jung, S., and Amit, I. (2014). Tissue-resident macrophage enhancer landscapes are shaped by the local microenvironment. Cell *159*, 1312–1326.

Liew, F.Y., Li, Y., and Millott, S. (1990). Tumor necrosis factor-α synergizes with IFN-γ in mediating killing of *Leishmania major* through the induction of nitric oxide. J. Immunol. *145*, 4306–4310.

Louis, C.A., Reichner, J.S., Henry, W.L., Jr., Mastrofrancesco, B., Gotoh, T., Mori, M., and Albina, J.E. (1998). Distinct arginase isoforms expressed in primary and transformed macrophages: regulation by oxygen tension. Am. J. Physiol. *274*, R775–R782.

Marino, M.W., Dunn, A., Grail, D., Inglese, M., Noguchi, Y., Richards, E., Jungbluth, A., Wada, H., Moore, M., Williamson, B., et al. (1997). Characterization of tumor necrosis factor-deficient mice. Proc. Natl. Acad. Sci. USA *94*, 8093–8098.

Mills, C.D., Kincaid, K., Alt, J.M., Heilman, M.J., and Hill, A.M. (2000). M-1/M-2 macrophages and the Th1/Th2 paradigm. J. Immunol. *164*, 6166–6173.

Morris, S.M., Jr. (2009). Recent advances in arginine metabolism: roles and regulation of the arginases. Br. J. Pharmacol. *157*, 922–930.

Munder, M., Choi, B.S., Rogers, M., and Kropf, P. (2009). L-arginine deprivation impairs *Leishmania major*-specific T-cell responses. Eur. J. Immunol. *39*, 2161–2172.

Murray, P.J., Allen, J.E., Biswas, S.K., Fisher, E.A., Gilroy, D.W., Goerdt, S., Gordon, S., Hamilton, J.A., Ivashkiv, L.B., Lawrence, T., et al. (2014). Macrophage activation and polarization: nomenclature and experimental guidelines. Immunity *41*, 14–20.

Nashleanas, M., Kanaly, S., and Scott, P. (1998). Control of *Leishmania major* infection in mice lacking TNF receptors. J. Immunol. *160*, 5506–5513.

Novosad, S.A., and Winthrop, K.L. (2014). Beyond tumor necrosis factor inhibition: the expanding pipeline of biologic therapies for inflammatory diseases and their associated infectious sequelae. Clin. Infect. Dis. *58*, 1587–1598.

Olekhnovitch, R., Ryffel, B., Müller, A.J., and Bousso, P. (2014). Collective nitric oxide production provides tissue-wide immunity during *Leishmania* infection. J. Clin. Invest. *124*, 1711–1722.

Ostuni, R., Piccolo, V., Barozzi, I., Polletti, S., Termanini, A., Bonifacio, S., Curina, A., Prosperini, E., Ghisletti, S., and Natoli, G. (2013). Latent enhancers activated by stimulation in differentiated cells. Cell *152*, 157–171.

Pauleau, A.L., Rutschman, R., Lang, R., Pernis, A., Watowich, S.S., and Murray, P.J. (2004). Enhancer-mediated control of macrophage-specific arginase I expression. J. Immunol. *172*, 7565–7573.

Pesce, J.T., Ramalingam, T.R., Mentink-Kane, M.M., Wilson, M.S., El Kasmi, K.C., Smith, A.M., Thompson, R.W., Cheever, A.W., Murray, P.J., and Wynn, T.A. (2009). Arginase-1-expressing macrophages suppress Th2 cytokine-driven inflammation and fibrosis. PLoS Pathog. *5*, e1000371.

Pfeffer, K., Matsuyama, T., Kündig, T.M., Wakeham, A., Kishihara, K., Shahinian, A., Wiegmann, K., Ohashi, P.S., Krönke, M., and Mak, T.W. (1993). Mice deficient for the 55 kd tumor necrosis factor receptor are resistant to endotoxic shock, yet succumb to *L. monocytogenes* infection. Cell *73*, 457–467.

Prajeeth, C.K., Haeberlein, S., Sebald, H., Schleicher, U., and Bogdan, C. (2011). *Leishmania*-infected macrophages are targets of NK cell-derived cytokines but not of NK cell cytotoxicity. Infect. Immun. *79*, 2699–2708.

Rada-Iglesias, A., Bajpai, R., Swigut, T., Brugmann, S.A., Flynn, R.A., and Wysocka, J. (2011). A unique chromatin signature uncovers early developmental enhancers in humans. Nature *470*, 279–283.

Reguera, R.M., Balaña-Fouce, R., Showalter, M., Hickerson, S., and Beverley, S.M. (2009). *Leishmania major* lacking arginase (ARG) are auxotrophic for polyamines but retain infectivity to susceptible BALB/c mice. Mol. Biochem. Parasitol. *165*, 48–56.

Riminton, S.D., Körner, H., Strickland, D.H., Lemckert, F.A., Pollard, J.D., and Sedgwick, J.D. (1998). Challenging cytokine redundancy: inflammatory cell movement and clinical course of experimental autoimmune encephalomyelitis are normal in lymphotoxin-deficient, but not tumor necrosis factor-deficient, mice. J. Exp. Med. *187*, 1517–1528.

Rutschman, R., Lang, R., Hesse, M., Ihle, J.N., Wynn, T.A., and Murray, P.J. (2001). Cutting edge: Stat6-dependent substrate depletion regulates nitric oxide production. J. Immunol. *166*, 2173–2177.

Sade-Feldman, M., Kanterman, J., Ish-Shalom, E., Elnekave, M., Horwitz, E., and Baniyash, M. (2013). Tumor necrosis factor-α blocks differentiation and enhances suppressive activity of immature myeloid cells during chronic inflammation. Immunity *38*, 541–554.

Serrat, N., Pereira-Lopes, S., Comalada, M., Lloberas, J., and Celada, A. (2012). Deacetylation of C/EBPβ is required for IL-4-induced arginase-1 expression in murine macrophages. Eur. J. Immunol. *42*, 3028–3037.

Sheldon, K.E., Shandilya, H., Kepka-Lenhart, D., Poljakovic, M., Ghosh, A., and Morris, S.M., Jr. (2013). Shaping the murine macrophage phenotype: IL-4 and cyclic AMP synergistically activate the arginase I promoter. J. Immunol. *191*, 2290–2298.

Stein, M., Keshav, S., Harris, N., and Gordon, S. (1992). Interleukin 4 potently enhances murine macrophage mannose receptor activity: a marker of alternative immunologic macrophage activation. J. Exp. Med. *176*, 287–292.

Tamoutounour, S., Guilliams, M., Montanana Sanchis, F., Liu, H., Terhorst, D., Malosse, C., Pollet, E., Ardouin, L., Luche, H., Sanchez, C., et al. (2013). Origins and functional specialization of macrophages and of conventional and monocyte-derived dendritic cells in mouse skin. Immunity *39*, 925–938.

Titus, R.G., Sherry, B., and Cerami, A. (1989). Tumor necrosis factor plays a protective role in experimental murine cutaneous leishmaniasis. J. Exp. Med. *170*, 2097–2104.

Tsunawaki, S., and Nathan, C.F. (1986). Macrophage deactivation. Altered kinetic properties of superoxide-producing enzyme after exposure to tumor cell-conditioned medium. J. Exp. Med. *164*, 1319–1331.

Tung Chen, Y., Perales, C., Lacruz, J., Senent, L., and Salavert, M. (2014). Visceral leishmaniasis infection during adalimumab therapy: a case report and literature review. Int. J. Rheum. Dis. *17*, 822–824.

Vassalli, P. (1992). The pathophysiology of tumor necrosis factors. Annu. Rev. Immunol. *10*, 411–452.

Vats, D., Mukundan, L., Odegaard, J.I., Zhang, L., Smith, K.L., Morel, C.R., Wagner, R.A., Greaves, D.R., Murray, P.J., and Chawla, A. (2006). Oxidative metabolism and PGC-1beta attenuate macrophage-mediated inflammation. Cell Metab. *4*, 13–24.

Wilhelm, P., Ritter, U., Labbow, S., Donhauser, N., Röllinghoff, M., Bogdan, C., and Körner, H. (2001). Rapidly fatal leishmaniasis in resistant C57BL/6 mice lacking TNF. J. Immunol. *166*, 4012–4019.

Witte, M.B., Barbul, A., Schick, M.A., Vogt, N., and Becker, H.D. (2002). Upregulation of arginase expression in wound-derived fibroblasts. J. Surg. Res. *105*, 35–42.

Wynn, T.A., Chawla, A., and Pollard, J.W. (2013). Macrophage biology in development, homeostasis and disease. Nature *496*, 445–455.

Yazdanpanah, B., Wiegmann, K., Tchikov, V., Krut, O., Pongratz, C., Schramm, M., Kleinridders, A., Wunderlich, T., Kashkar, H., Utermöhlen, O., et al. (2009). Riboflavin kinase couples TNF receptor 1 to NADPH oxidase. Nature *460*, 1159–1163.